AIAA Infotech@Aerospace Conference
and
AIAA Unmanned...Unlimited Conference
6 - 9 April 2009, Seattle, Washington

AIAA 2009-2018

An Analytic Trajectory Planner for Aircraft with Severe Damage or Failures

Hee Jun Choi* and Ella M. Atkins†
University of Michigan, Ann Arbor, MI 48105

This paper describes an analytic real-time emergency landing trajectory planner applicable in situations where an aircraft experiences severe damage or failure(s) that contract the feasible lateral plane flight envelope. Solutions are constructed as sequences of spirals that follow a reference arc, extending a traditional Dubins path solver to handle cases in which an aircraft cannot fly straight. A comprehensive Turning Dubins Vehicle (TDV) solver is presented to handle the spectrum of relative distances and headings between aircraft initial state and the landing runway approach end. This solver is shown to generate minimum-distance landing paths. Example solutions are presented with future work aimed at assessing the impact of transitions and disturbances as well as application to specific damage/failure scenarios.

Nomenclature

σ	Curve for the Turning Dubins Vehicle (TDV)
$\mathcal{O}$	Circular curve for the TDV
a	Circular arc curve for the TDV
b	Product of circular arc curves
Σ	Set of possible curves for the TDV
Σ_c	Set of circular curves for the TDV
$\mathcal{A}$	Set of circular arc curves for the TDV
$\mathcal{A}_r$	Set of possible reference arcs connecting two centers of the initial and final circular curves
$\mathcal{B}$	Set of possible sequences of two different turning radii for the TDV
$\vec{V}$	Velocity vector
$\vec{K}$	Curvature vector
r	Radius of circular curve
δ	Central angle of the reference arc
ρ	Central angle of the circular flight path arc
τ	Opposite central angle of the circular flight path arc subtending $2\pi - \rho$
l	Length of flight path arc curves
l_J	Length of the reference arc traversed over $(n-1)$ arc pair sequences
J	Length of the reference arc traversed over two-arc sequence
n	Number of arc sequences in $\mathcal{B}$
n_m	Minimum number of arc sequences in $\mathcal{B}$
λ	Distance of the points of a straight line from a known point

Subscript

r	Reference arc
1	First circular curve of two different radius circular curves
2	Second circular curve of two different radius circular curves
m	Minimum radius turning circle
M	Maximum radius turning circle

*Research Assistant, Aerospace Engineering, University of Michigan, Ann Arbor, MI 48105
†Associate Professor, Aerospace Engineering, University of Michigan, Ann Arbor, MI 48105, Associate Fellow

I. Introduction

Modern aircraft operate safely over a variety of conditions. Flight management systems capably monitor onboard systems and are expanding to reliably react in environments made challenging by adverse weather and/or traffic conditions. Certified autopilot systems, however, continue to presume a constant, known flight performance envelope, applying fixed guidance and control laws for each flight mode. When sustaining damage or experiencing failures, an aircraft's flight envelope will typically contract. Researchers have developed adaptive control laws to maintain stability and system identification methods to characterize degraded aircraft dynamics, but flight planning and guidance tasks still revert to the human pilot since fixed envelope assumptions no longer apply. In previous work,[1–3] we developed an adaptive flight planning capability that automatically ranked and selected a nearby landing runway and built a trajectory to that runway under the assumption that either a Dubins path solution could be found or that sufficient flight planning time existed to identify a landing trajectory via search over sequences of feasible trim states. The search-based planner, however, often required nontrivial time (more than a minute in some cases) to identify a solution, during which time it was assumed the aircraft could remain stably aloft. This paper describes an extension to the Dubins path landing solution that enables a feasible landing trajectory to be generated even when straight flight is not possible. This solution requires only that the aircraft be capable of left or right turns of two different turning radii, enabling analytic construction of a sequence of spirals between initial state and the approach end of the landing runway. Scenarios in which the aircraft cannot maintain straight flight can result from a variety of conditions such as structural damage (e.g., to a wing) or actuator failures (e.g., stuck, fully-deflected rudder or ailerons).

Other researchers have begun to design flight management architectures that will assist the pilot in decision-making during emergencies.[4] Researchers have also studied the aircraft trajectory planning problem for a variety of applications, including recent work on sequencing circular segments to allow a laser to consistently track a target.[5] The classic engine-out (loss-of-thrust) scenario was addressed in our previous work by an extension of a Dubins path solver[1] and has also been studied in the context of a turn-back landing cast in an optimal control framework.[6] There also have been efforts to design multi-layer autonomous flight management systems for Unmanned Air Systems (UAS) such as the multi-layer intelligent control architecture.[7] We have previously modeled emergency situations ranging from loss of thrust[1] to actuator failures[2] to a commercial transport with severe left wing damage.[3] This work adopts the same framework as was introduced in our previous work,[1] as shown in Figure 1. In the presence of failures and/or damage, the emergency flight planner activates the adaptive flight planner through a variable autonomy pilot interface and flight plan monitor. Within the AFP, a Landing Site Search (LSS) module determines a safe landing site, currently a runway deemed feasible based on length, width, wind conditions, etc.[1] The Segmented Trajectory Planner constructs a sequence of valid post-failure trim states to this landing site. This paper presents an analytic trajectory planner that extends the analytic Dubins solver proposed for nominal or loss-of-thrust scenarios thus reduces the requirement to use the computationally-intensive search-based solver. The remainder of this article is organized as follows. Section II describes the geometric constraints required to connect the initial turning flight segment with the final turn to touchdown. Section III presents the conditions under which the landing runway can be reached. Section IV describes the minimum-length trajectory plan for a case in which an aircraft experiences severe wing damage. Section V provides example landing trajectories, while section VI presents conclusions and future work.

II. Sequence of Spirals Geometric Analysis

To extend the Dubins path landing solution, we first define the concept of a Turning Dubins Vehicle.

Definition *(Turning Dubins Vehicle (TDV))* A Turning Dubins Vehicle (TDV) is a planar vehicle that is constrained to move along paths of curvature bounded both above and below, without reversing direction and maintaining a constant speed.

Let $\sigma : [0, T] \to \mathbb{R}^2$ be a curve for the TDV that is twice differentiable for maneuver times $T > 0$. For TDV velocity $\vec{V}$ and unit tangent $\vec{T} = \frac{\vec{V}}{\|\vec{V}\|}$, the curvature vector $\vec{K}$ is defined as the rate of change of $\vec{T}$ with

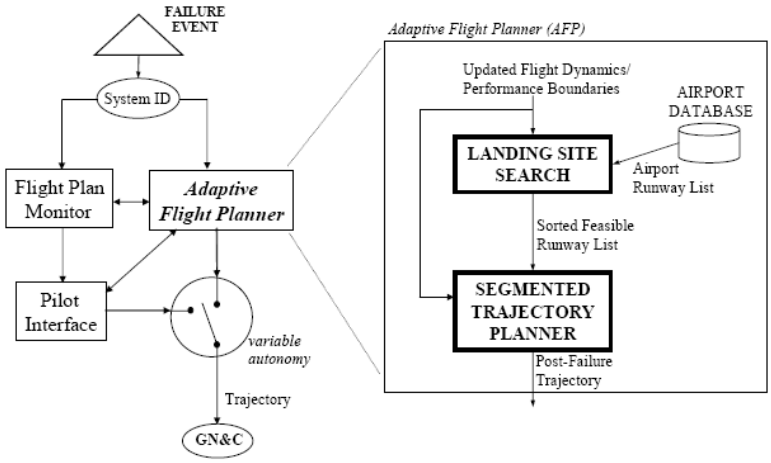

Figure 1. Emergency Flight Management Architecture.

respect to arc length s:

$$\vec{K} = \frac{d\vec{T}}{ds} = \frac{1}{\|\vec{V}\|}\dot{\vec{T}} \tag{1}$$

$$K = \|\vec{K}\| = \frac{1}{r} \tag{2}$$

where r is the turning circle radius. Since $r_m \leq r \leq r_M$ where r_m is the minimum turning radius and r_M is the maximum turning radius, the magnitude of the curvature of σ is bounded above by $\frac{1}{r_m}$ and bounded below by $\frac{1}{r_M}$. Let Σ represent the set of possible curves for the TDV, i.e., $\Sigma = \left\{\sigma | K \in \left[\frac{1}{r_M}, \frac{1}{r_m}\right]\right\}$.

Since our landing solution requires only left or right turns of two different radii, we shall use $\mathcal{O}$ to denote a circle. Given a center c in $\mathbb{R}^2$, a radius r, and a sign of the turning rate $sgn\left(\dot{\psi}\right)$, let $\mathcal{O}\left(c, r, sgn\left(\dot{\psi}\right)\right) : [0, T_{\mathcal{O}}] \rightarrow \mathbb{R}^2$ represent a circle of radius r with center c and direction of motion $sgn\left(\dot{\psi}\right)$ where $T_{\mathcal{O}}$ denotes the maneuver time during $\mathcal{O}$ and let Σ_c be the set of circular curves for the TDV as follows:

$$\Sigma_c = \left\{ \mathcal{O}\left(c, r, sgn\left(\dot{\psi}\right)\right) | r_m \leq r \leq r_M, sgn\left(\dot{\psi}\right) = \left\{ \begin{array}{ll} + & \text{if } \dot{\psi} > 0 \\ - & \text{if } \dot{\psi} < 0 \end{array} \right\} \right. \tag{3}$$

To obtain the landing trajectory, we identify a reference arc that can be followed by alternating segments of two different turning radii that include a predefined safety factor sufficient for disturbance rejection. For a given center c in $\mathbb{R}^2$ and two given points p_i and p_f in $\mathbb{R}^2$, let $a\left(c, p_i, p_f\right) : [0, T_a] \rightarrow \mathbb{R}^2$ be a circular arc connecting p_i and p_f with arc center c and let $\mathcal{A} = \left\{a\left(c, p_i, p_f\right) | c, p_i, p_f \in \mathbb{R}^2\right\}$. As shown in Figure 2, $\mathcal{O}_i$ and $\mathcal{O}_f$ in Σ_c represent the initial and final circular curves, respectively, and would formerly have represented the initial and final arcs from which a connecting (straight) tangent would have been computed for a Dubins path solution. $\mathcal{O}_f$ is tangent to an extension line from the runway, guiding the aircraft to the desired touchdown state at the landing runway's approach end. The curvature vector $\vec{K}$ is orthogonal to $\vec{T}$ when $\vec{T}$ is on the circle. Let $\vec{r}_E = \frac{1}{2}\left(\vec{r}_{c_i} + \vec{r}_{c_f}\right)$. As shown in Figure 2, since $\triangle Oc_iE$ and $\triangle Oc_fE$ are congruent, the centers of the reference arc a_r lie on a straight line passing through E and F. In order to find a vector $\vec{K}_O$ that

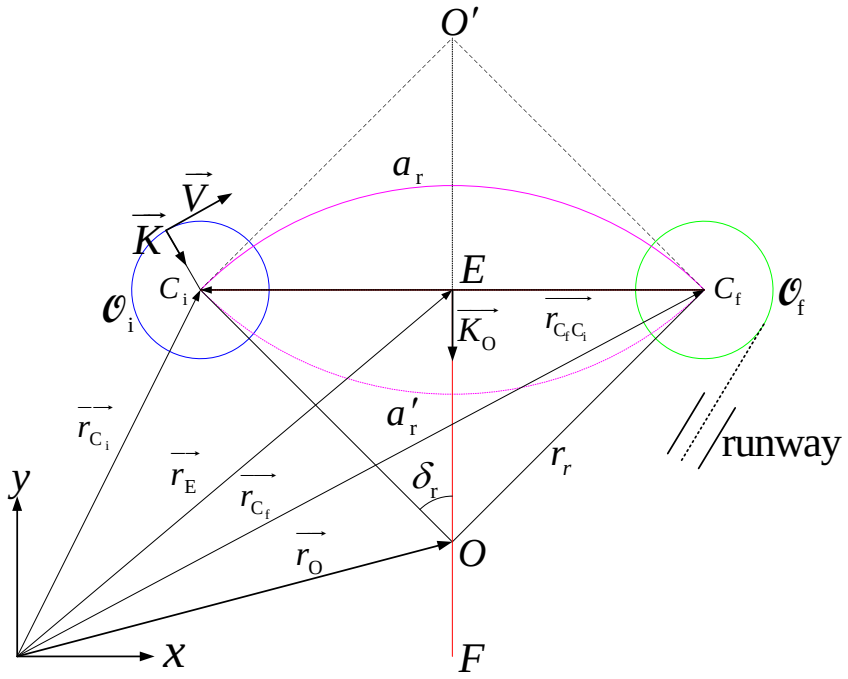

Figure 2. Arcs Connecting Initial and Final Approach Turns

represents straight line $\overline{EF}$ perpendicular to $\vec{r}_{c_f c_i}$, we represent curvature vector $\vec{K}$ in polar coordinates :

$$\vec{K}_i = \begin{bmatrix} K\cos\zeta_i \\ K\sin\zeta_i \end{bmatrix} \tag{4}$$

Let $\vec{r}_{c_f c_i} = \begin{bmatrix} x_{c_f c_i} \\ y_{c_f c_i} \end{bmatrix}$. Since $\vec{K}_O$ is perpendicular to $\vec{r}_{c_f c_i}$,

$$\vec{K}_O \cdot \vec{r}_{c_f c_i} = x_{c_f c_i} K\cos\zeta_O + y_{c_f c_i} K\sin\zeta_O = 0 \tag{5}$$

$$\zeta_O = \arctan\left(-\frac{x_{c_f c_i}}{y_{c_f c_i}}\right) \tag{6}$$

Hence, $\vec{r}_O$ to the center O of the arc is given by

$$\vec{r}_O = \vec{r}_E + \lambda\vec{K}_O \tag{7}$$

where λ has a range from $-\infty$ to ∞ and $\vec{K}_O = \begin{bmatrix} K\cos\zeta_O \\ K\sin\zeta_O \end{bmatrix}$. Furthermore, since $\triangle O c_f c_i$ and $\triangle O' c_f c_i$ are congruent, there also exists a dual reference arc, a'_r, as shown in Figure 2. Hence, we can choose one of the two arcs according to travel direction $sgn\left(\dot{\psi}\right)$ around the turning circle. Let $\mathcal{A}_r$ be the set of possible reference arcs connecting centers c_i and c_f as follows :

$$\mathcal{A}_r = \left\{ a\left(O, c_i, c_f\right) | \vec{r}_O = \frac{1}{2}\left(\vec{r}_{c_i} + \vec{r}_{c_f}\right) + \lambda\vec{K}_O, \quad -\infty \le \lambda \le \infty \right\} \tag{8}$$

By using $\vec{r}_{Oc_i}$, we can calculate the radius r_r, angle δ_r, and length $l_r$of the reference arc $a_r \in \mathcal{A}_r$, as shown in Figure 2:

$$r_r = \|\vec{r}_{Oc_i}\| \tag{9}$$

$$\delta_r = \begin{cases} \arccos\left(\frac{\vec{r}_{Oc_i}\cdot(\vec{r}_E-\vec{r}_O)}{\|\vec{r}_{Oc_i}\|\|\vec{r}_E-\vec{r}_O\|}\right) & \text{if} \quad 0 \le \lambda \le \infty \\ \pi - \arccos\left(\frac{\vec{r}_{Oc_i}\cdot(\vec{r}_E-\vec{r}_O)}{\|\vec{r}_{Oc_i}\|\|\vec{r}_E-\vec{r}_O\|}\right) & \text{if} \quad -\infty \le \lambda < 0 \end{cases} \tag{10}$$

$$l_r = 2r_r\delta_r \tag{11}$$

If $a_{2i-1}(T_{2i-1}) = a_{2i}(0)$ where a_{2i-1} and a_{2i} are the arcs of $\mathcal{O} \in \Sigma_c$ intercepted by $a_r \in \mathcal{A}_r$, then we define a product of two arcs as :

$$b_i = a_{2i-1} * a_{2i} = \begin{cases} a_{2i-1}(t - T_{2i-2}), & T_{2i-2} \le t \le T_{2i-1} \\ a_{2i}(t - T_{2i-1}), & T_{2i_1} \le t \le T_{2i} \end{cases} \tag{12}$$

where $T_0 = 0$.

Theorem II.1 *Let $\mathcal{O}_1\left(c_1, r_1, sgn\left(\dot{\psi}\right)\right)$ and $\mathcal{O}_2\left(c_2, r_2, sgn\left(\dot{\psi}\right)\right)$ be in Σ_c with $r_1 \neq r_2$. Let a_1 be the intercepted arc of $\mathcal{O}_1$ with $a_r \in \mathcal{A}_r$ and center c_1 such that $a_1(c_1, p_0, p_1) : [0, T_1] \to \mathbb{R}^2$ where p_0 and p_1 lie on a_r. Let a_2 be the intercepted arc of $\mathcal{O}_2$ with $a_r \in \mathcal{A}_r$ and center c_2. Suppose c_1 lies on arc a_r. If c_2 is located on straight line $\overline{p_1c_1}$ with distance r_2 from p_1, then $\mathcal{O}_1$ and $\mathcal{O}_2$ are tangent. Moreover, the change in heading angle of a TDV over $a_1 * a_2$ is either $2\pi + 4\delta_1 - 2\delta_2$ or $2\pi - 4\delta_1 + 2\delta_2$ according to $sgn\left(\dot{\psi}\right)$ where $\delta_1 = \arcsin\left(\frac{r_1}{2r_r}\right)$ and $\delta_2 = \arccos\left(\frac{\vec{a}_{Oc_2}\cdot\vec{a}_{Op_1}}{\|\vec{a}_{Oc_2}\|r_r}\right)$.*

Proof Assume c_2 is on straight line $\overline{p_1c_1}$ with distance r_2 from p_1. Then, the TDV velocity, $\vec{V}$, is perpendicular to $\vec{r}_{p_1c_1}$ at p_1. Since c_2 is located on the straight line $\overline{p_1c_1}$, $\vec{r}_{p_1c_1}$ and $\vec{r}_{p_1c_2}$ are parallel, and $\vec{V}$ is perpendicular to $\vec{r}_{p_1c_2}$ at p_1. Hence, $\mathcal{O}_1$ and $\mathcal{O}_2$ are tangent.
Since $\mathcal{O}_1$ and $\mathcal{O}_2$ are tangent at p_1, $a_1(T_1) = a_2(0) = p_1$, i.e. $a_2(c_2, p_1, p_2) : [0, T_2] \to \mathbb{R}^2$ where p_1 and p_2 lie on a_r. Hence, the product of two arcs $a_1 * a_2$ is defined. Given the assumption $r_1 \neq r_2$, $r_1 > r_2$ or $r_1 < r_2$, as shown in Figure 3 for $i = 1$. For both cases, $\triangle Oc_2p_1$ and $\triangle Oc_2p_2$ are congruent where p_2 is another intersection point of $\mathcal{O}_2$ and $a_r \in \mathcal{A}_r$. Since $\angle Op_1c_1$ is $\frac{\pi}{2} - \delta_1$, the central angles of $\mathcal{O}_2$ including τ_2 and ρ_2 are given by :

$$\tau_2 = \pi + 2(\delta_1 - \delta_2) \tag{13}$$

$$\rho_2 = 2\pi - \tau_2 \tag{14}$$

Since $\triangle Op_1c_1$ is an isosceles triangle, the central angles of $\mathcal{O}_1$ including τ_1 and ρ_1 are given by :

$$\tau_1 = \pi - 2\delta_1 \tag{15}$$

$$\rho_1 = \pi + 2\delta_1 \tag{16}$$

We now determine angles δ_1 and δ_2. Since $\triangle Op_1c_1$ is an isosceles triangle,

$$\delta_1 = \arcsin\left(\frac{r_1/2}{r_r}\right) \tag{17}$$

Note that the length of the arc a_r intercepted by $\mathcal{O}_1$, l_1, is $4r_r\delta_1$. To compute δ_2, define $\vec{r}_{Op_1}$ as a vector from $\vec{r}_{Oc_1}$ rotated $-4\delta_1$ about the z axis:

$$\vec{r}_{Op_1} = \begin{bmatrix} \cos(-4\delta_1) & -\sin(-4\delta_1) \\ \sin(-4\delta_1) & \cos(-4\delta_1) \end{bmatrix} \vec{r}_{Oc_1} \tag{18}$$

Since $\vec{r}_{p_1c_2} = \frac{r_2}{r_1}\vec{r}_{p_1c_1}$ and $\vec{r}_{Oc_2} = \vec{r}_{Op_1} + \vec{r}_{p_1c_2}$,

$$\therefore \delta_2 = \arccos\left(\frac{\vec{r}_{Oc_2}\cdot\vec{r}_{Op_1}}{\|\vec{r}_{Oc_2}\|r_r}\right) \tag{19}$$

Note that the length of the arc of a_r intercepted by $\mathcal{O}_2$, l_2, is $2r_r\delta_2$. Since the TDV doesn't reverse direction, we only consider two permutations about central angles of $\mathcal{O}_1$ and $\mathcal{O}_2$ according to $sgn\left(\dot{\psi}\right)$:

$$\{\rho_1, \tau_2\} \quad \text{or} \quad \{\tau_1, \rho_2\} \tag{20}$$

Hence, the change in heading angle of the TDV in $a_1 * a_2$ is given by:

$$2\pi + 4\delta_1 - 2\delta_2 \quad \text{for} \quad \{\rho_1, \tau_2\} \tag{21}$$

$$2\pi - 4\delta_1 + 2\delta_2 \quad \text{for} \quad \{\tau_1, \rho_2\} \tag{22}$$

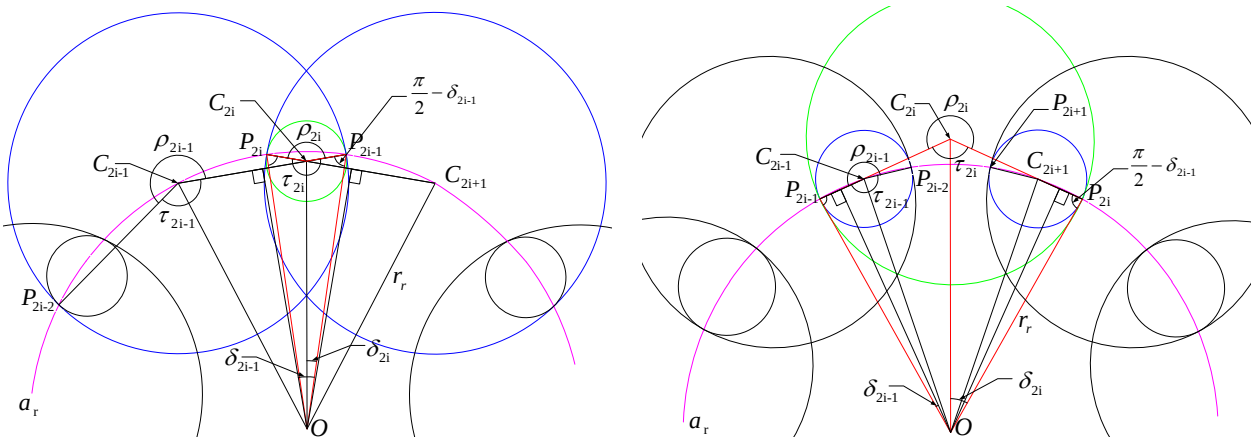

(a) $r_{2i-1} > r_{2i}$ (b) $r_{2i-1} < r_{2i}$

Figure 3. Product of n arcs

Corollary II.2 *Let* $\mathcal{O}_{2i-1}\left(c_{2i-1}, r_{2i-1}, sgn\left(\dot{\psi}\right)\right)$ *and* $\mathcal{O}_{2i}\left(c_{2i}, r_{2i}, sgn\left(\dot{\psi}\right)\right)$ *be in* Σ_c *with* $r_{2i-1} \neq r_{2i}$ *and* $r_i = r_{i+2}$ *for all* $i \in \mathbb{N}$. *Let* a_1 *be the intercepted arc of* $\mathcal{O}_1$ *with* $a_r \in \mathcal{A}_r$ *and center* c_1 *such that* $a_1(c_1, p_0, p_1) : [0, T_1] \to \mathbb{R}^2$ *where* p_0 *and* p_1 *lie on* a_r. *Suppose* c_1 *lies on* a_r. *If* c_{2i} *is located on straight line* $\overline{p_{2i-1}c_{2i-1}}$ *with distance* r_2 *from* p_{2i-1} *and* c_{2i+1} *is located on straight line* $\overline{p_{2i}c_{2i}}$ *with distance* r_1 *from* p_{2i} *for all* $i \in \mathbb{N}$ *where* p_{2i-1} *and* p_{2i} *lie on* a_r, *then* $\mathcal{O}_{2i-1}$ *and* $\mathcal{O}_{2i}$ *are tangent at* p_{2i-1}, *and* $\mathcal{O}_{2i}$ *and* $\mathcal{O}_{2(i+1)-1}$ *at* p_{2i} *exist such that* c_{2i-1} *and* $c_{2(i+1)-1}$ *lie on* a_r *for all* $i \in \mathbb{N}$. *Moreover, the change in heading angle of the TDV over* $\{b_i | i \in \{1, 2, \cdots, n\}\}$ *is either* $n(2\pi + 4\delta_1 - 2\delta_2)$ *or* $n(2\pi - 4\delta_1 + 2\delta_2)$ *where* $\delta_1 = \arcsin\left(\frac{r_1/2}{r_r}\right)$ *and* $\delta_2 = \arccos\left(\frac{\vec{a}_{Oc_2} \cdot \vec{a}_{Op_1}}{\|\vec{a}_{Oc_2}\| r_r}\right)$.

Proof Suppose c_{2i} is located on straight line $\overline{p_{2i-1}c_{2i-1}}$ with distance r_2 from p_{2i-1} and c_{2i+1} is located on straight line $\overline{p_{2i}c_{2i}}$ with distance r_1 from p_{2i} where p_{2i-1} and p_{2i} lie on a_r for all $i \in \mathbb{N}$. Since c_1 lies on a_r, $\mathcal{O}_1$ and $\mathcal{O}_2$ are tangent at p_1 and the product of two arcs $a_1 * a_2$ is defined such that $a(c_2, p_1, p_2) : [0, T_2] \to \mathbb{R}^2$ where p_1 and p_2 lie on a_r from Theorem II.1. Since the perperndicular bisector of a chord contains the center of the circle, $\triangle Oc_2p_1$ and $\triangle Oc_2p_2$ are congurent, and $\angle Op_2c_2 = \angle Op_1c_2$. By triangle congruence, $\overline{Oc_3} = r_r$, and c_3 lies on a_r. Since the velocity of the TDV, $\vec{V}$, is perpendicular to $\vec{r}_{p_2c_2}$ and $\vec{r}_{p_2c_3}$ at p_2, $\mathcal{O}_2$ and $\mathcal{O}_3$ are tangent.

Let the nth proposition be that $\mathcal{O}_{2n-1}$ and $\mathcal{O}_{2n}$ are tangent at p_{2n-1}, and $\mathcal{O}_{2n}$ and $\mathcal{O}_{2n+1}$ at p_{2n} exist such that c_{2n-1} and c_{2n+1} lie on a_r. Suppose our nth proposition is true. From Theorem II.1, $\mathcal{O}_{2n+1}$ and $\mathcal{O}_{2n+2}$ are tangent at p_{2n+1} because c_{2n+1} lies on a_r. Since $\triangle Op_{2n+1}c_{2n+1}$ and $\triangle Op_{2n+2}c_{2n+3}$ are congruent, c_{2n+3} lies on a_r, and $\mathcal{O}_{2n+2}$ and $\mathcal{O}_{2n+3}$ are tangent at p_{2n+2}.

Since $\mathcal{O}_{2i-1}$ and $\mathcal{O}_{2i}$ are tangent at p_{2i-1} for all $i \in \mathbb{N}$, $a_{2i-1}(T_{2i-1}) = a_{2i}(0) = p_{2i-1}$, and b_i is defined for all $i \in \mathbb{N}$. If $b_i(T_2 i) = b_{i+1}(0)$ where $b_i = a_{2i-1} * a_{2i}$ and $b_{i+1} = a_{2(i+1)-1} * a_{2(i+1)}$, then we define a product of two products as :

$$b_i * b_{i+1} = \begin{cases} b_i(t - T_{2i-2}), & T_{2i-2} \leq t \leq T_{2i} \\ b_{i+1}(t - T_{2i}), & T_{2i} \leq t \leq T_{2i+2} \end{cases} \tag{23}$$

where $T_0 = 0$. Since $\mathcal{O}_{2i}$ and $\mathcal{O}_{2(i+1)-1}$ are tangent at p_{2i} for all $i \in \mathbb{N}$, $b_1 * b_2 * \cdots * b_n$ is defined for all $i \in \mathbb{N}$. Let $\mathcal{B}$ represent the set of possible sequences of two different turning radii for the TDV in $a_r \in \mathcal{A}_r$, i.e. $\mathcal{B} = \{b_i | i \in \{1, 2, \cdots, n\}\}$ over a_r.
For $n = 1$, it is true from Theorem II.1 that the change in heading angle of the TDV in b_1 is either $2\pi - 4\delta_1 - 2\delta_2$ or $2\pi - 4\delta_1 + 2\delta_2$ according to $sgn\left(\dot{\psi}\right)$. Suppose our nth proposition is true. Since $\mathcal{O}_{2n}$ and $\mathcal{O}_{2(n+1)-1}$ are tangent at p_{2n} and $c_{2(n+1)-1}$ lies on a_r, the change in heading angle of the TDV in b_{n+1} defined by $\mathcal{O}_{2(n+1)-1}$ and $\mathcal{O}_{2(n+1)}$ is $2\pi + 4\delta_1 - 2\delta_2$ or $2\pi - 4\delta_1 + 2\delta_2$ according to $sgn\left(\dot{\psi}\right)$. Hence, the $(n+1)$th proposition is true. By induction, the change in heading angle of the TDV in $\{b_i | i \in \{1, 2, \cdots, n\}\}$ for all $n \in \mathbb{N}$ is either $n\left(2\pi + 4\delta_1 - 2\delta_2\right)$ or $n\left(2\pi - 4\delta_1 + 2\delta_2\right)$ according to $sgn\left(\dot{\psi}\right)$.

III. Landing Trajectory Feasibility Condition

In this section, we present criteria by which a particular landing site is feasible(reachable) with a TDV trajectory about reference arc a_r. From Corollary II.2, $\mathcal{B} = \{b_i | i \in \{1, 2, \cdots, n\}\}$ over $a_r \in \mathcal{A}_r$. After n sequences, however, $\mathcal{O}_f$ and $\mathcal{O}_{2n}$ are not guaranteed tangent. The following theorem describes the feasibility condition about a_r for the TDV to reach the selected runway.

Theorem III.1 *Consider $\mathcal{B} = \{b_i | i \in \{1, 2, \cdots, n\}\}$ over $a_r \in \mathcal{A}_r$. Let $\mathcal{O}_1$ and $\mathcal{O}_f$ represent the initial and final circular curves, respectively. Then there exists an a_r such that $\mathcal{O}_f$ and $\mathcal{O}_{2n}$ are tangent at p_{2n} if and only if r_r satisfies the feasibility condition :*

$$\delta_r - n\left|2\delta_1 - \delta_2\right| = 0 \tag{24}$$

where $\delta_r = \begin{cases} \arcsin\left(\frac{\|\vec{r}_{C_f c_i}\|}{2r_r}\right) & \text{if} \quad 0 \le \lambda \le \infty \\ \pi - \arcsin\left(\frac{\|\vec{r}_{C_f c_i}\|}{2r_r}\right) & \text{if} \quad -\infty \le \lambda < 0 \end{cases}$, $\delta_1 = \arcsin\left(\frac{r_1}{2r_r}\right)$, *and* $\delta_2 = \arctan\left(\frac{\sqrt{r_r^2 - \frac{r_1^2}{4}}}{\frac{r_r^2}{r_2} - \frac{r_1}{2}}\right)$.
Hence, the TDV can reach the selected runway.

Proof Suppose there exists an a_r such that $\mathcal{O}_f$ and $\mathcal{O}_{2n}$ are tangent at p_{2n}. Hence, $\mathcal{O}_f$ is the additional circular curve, i.e., $\mathcal{O}_{2n+1}$, such that $\mathcal{O}_{2n}$ and $\mathcal{O}_{2n+1}$ are tangent at p_{2n}. Considering the imaginary $\mathcal{O}_{2n+2}$ such that $\mathcal{O}_{2n+1}$ and $\mathcal{O}_{2n+2}$ are tangent, we can define an additional segment $b_{n+1} \in \{b_i | i \in \mathbb{N}\}$ over a_r. From Corollary II.2, the change in heading angle of the TDV over each b_i is identical except case b_1, and the length of $a_r \in \mathcal{A}_r$ traversed over each b_i is also identical except case b_1. Note that the change in heading angle of the TDV over b_1 is different because of the TDV's initial position, p_0.
Let J represent the length of $a_r \in \mathcal{A}_r$ traversed over each b_i for all $i \in \{2, 3, \cdots, n\}$ and l_J represent the length of a_r traversed over $\{b_i | i \in \{2, 3, \cdots, n\}\}$. Since J is independent of $i \in \{2, 3, \cdots, n\}$,

$$l_J = (n-1)\, J \tag{25}$$

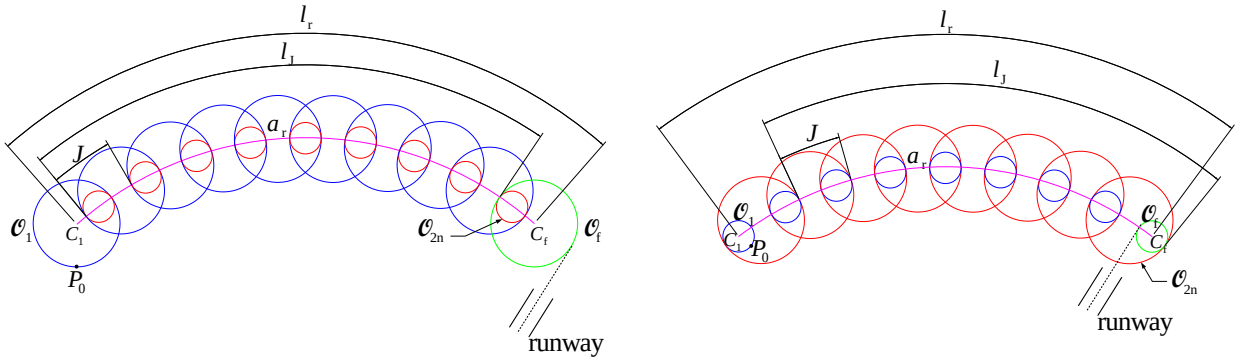

(a) $r_1 > r_2$ (b) $r_1 < r_2$

Figure 4. Feasibility Condition

where $n \in \mathbb{N}$. Hence, l_J must be an integer multiple of J for the runway to be reached via $\{b_i | i \in \{1, 2, \cdots, n\}\}$. From Theorem II.1, l_1 and l_2 represent the length of $a_r \in \mathcal{A}_r$ traversed over each a_{2i-1} and a_{2i}, respectively, such that $b_i = a_{2i-1} * a_{2i}$ for all $i \in \{2, 3, \cdots, n\}$, and are defined as :

$$l_1 = 4r_r\delta_1 \qquad \text{and} \qquad l_2 = 2r_r\delta_2 \tag{26}$$

From Eq. 25, $l_J = l_r - |l_1 - l_2|$, and $J = |l_1 - l_2|$. Substituting Eqs. 11 and 26, the feasibility condition for $a_r \in \mathcal{A}_r$ can be determined:

$$\delta_r - n\,|2\delta_1 - \delta_2| = 0 \tag{27}$$

where $\delta_r = \begin{cases} \arcsin\left(\frac{\|\vec{r}_{C_f c_i}\|}{2r_r}\right) & \text{if} \quad 0 \le \lambda \le \infty \\ \pi - \arcsin\left(\frac{\|\vec{r}_{C_f c_i}\|}{2r_r}\right) & \text{if} \quad -\infty \le \lambda < 0 \end{cases}$, $\delta_1 = \arcsin\left(\frac{r_1}{2r_r}\right)$, and $\delta_2 = \arctan\left(\frac{\sqrt{r_r^2 - \frac{r_1^2}{4}}}{\frac{r_r^2}{r_2} - \frac{r_1}{2}}\right)$.

Note that $l_1 > l_2$ if $r_1 > r_2$ and $l_1 < l_2$ if $r_1 < r_2$, and $r_{2i-1} \neq r_{2i}$ and $r_i = r_{i+2}$ in $\mathcal{O}_{2i-1}\left(c_{2i-1}, r_{2i-1}, sgn\left(\dot{\psi}\right)\right)$ and $\mathcal{O}_{2i}\left(c_{2i}, r_{2i}, sgn\left(\dot{\psi}\right)\right)$ for all $i \in \mathbb{N}$. Since $\mathcal{O}_f$ and $\mathcal{O}_{2n}$ are tangent at p_{2n}, the TDV can reach the selected runway. Suppose r_r satisfies the feasibility condition in Eq. 24.

$$\therefore l_J = (n-1)\,J \tag{28}$$

Since the length of $a_r \in \mathcal{A}_r$ traversed over each b_i is identical except the case in b_1, we take a_r such that $l_J = (n-1)\,J$. Since l_J is the length of a_r from p_2 to p_{2n} from the definition, $\mathcal{O}_{2n}$ and $\mathcal{O}_{2n+1}$ are tangent at p_{2n}, and c_{2n+1} lies on a_r by Corollary II.2. When $r_1 > r_2$, the sum of the length of a_r from c_1 to p_2 and the length of a_r from p_{2n} to c_{2n+1} is J, and the length of a_r from c_1 to c_{2n+1} is l_r. Moreover, when $r_1 < r_2$, the difference of the length of a_r from c_1 to p_2 and the length of a_r from c_{2n+1} to p_{2n} is J, and the length of a_r from c_1 to c_{2n+1} is l_r. Since l_r is the length of a_r from c_1 to c_f from the definition, c_{2n+1} is c_f, and c_{2n} and c_f are tangent at p_{2n}. Hence, the selected runway can be reached. Note that if $r_1 < r_2$, p_1 is located on the extension arc from c_1 in $a_1\,(c_1, p_0, p_1)$.

In Figure 5, we specify a waypoint generation algorithm (WGA) aimed at a practical, real-time solution that extends our previous Dubins path strategy[1] to cases in which straight flight is not feasible. If straight flight is possible, the existing segmented trajectory planner constructs a Dubins path of guaranteed minimum length to the top-ranked landing runway.[1] Otherwise, we adopt the lateral plane trajectory of alternating-radius turns described in this paper, with flight path angle set to a value that ensures touchdown at the runway altitude.[a] We define the initial and final turning circle centers, from which the set of feasible reference arcs can be determined as described below.

IV. Analytic Determination of the Minimum Turning Sequence

Since λ has range $-\infty$ to ∞ in $\mathcal{A}_r$, we can find a lower bound for n in $\{b_i | i \in \{1, 2, \cdots, n\}\}$ as shown in Figure 6. $\mathcal{A}_r$ evolves from a straight line to a circle as λ is varied from ∞ to $-\infty$. Moreover, since our landing solution requires only left or right turns of two different radii and $r_m \le r \le r_M$, J is bounded. Let n_m represent the minimum value of n such that J has the maximum value satisfying the feasibility condition, and let a_{r_m} represent the reference arc having n_m.

Theorem IV.1 *Consider $\mathcal{B} = \{b_i | i \in \{1, 2, \cdots, n\}\}$ over $a_r \in \mathcal{A}_r$. Let $\mathcal{O}_1$ and $\mathcal{O}_f$ represent the initial and final circular curves, respectively. If $l_r = nJ$, then $n_m = \lceil \frac{\|\vec{r}_{c_f c_i}\|}{|2r_1 - 2r_2|} \rceil$ and there exists a_{r_m} such that $\mathcal{O}_{2n}$ and $\mathcal{O}_f$ are tangent at p_{2n} where*

$$r_1 = r_M \quad \text{and} \quad r_2 = r_m \quad \text{if} \quad r_1 > r_2 \tag{29}$$

$$r_1 = r_m \quad \text{and} \quad r_2 = r_M \quad \text{if} \quad r_1 < r_2 \tag{30}$$

Proof Suppose $l_r = nJ = n\,|l_1 - l_2|$. From the definition of $\mathcal{A}_r$, $\mathcal{A}_r$ evolves from a straight line to a circle as λ is varied from ∞ to $-\infty$. Hence, $\|\vec{r}_{c_f c_i}\| \le l_r$.

$$\frac{\|\vec{r}_{c_f c_i}\|}{|l_1 - l_2|} \le n \tag{31}$$

[a] For simplicity we currently presume the damage/failure does not compromise the aircraft's ability to command nominal descending flight path angles γ for the sequenced turning segments.

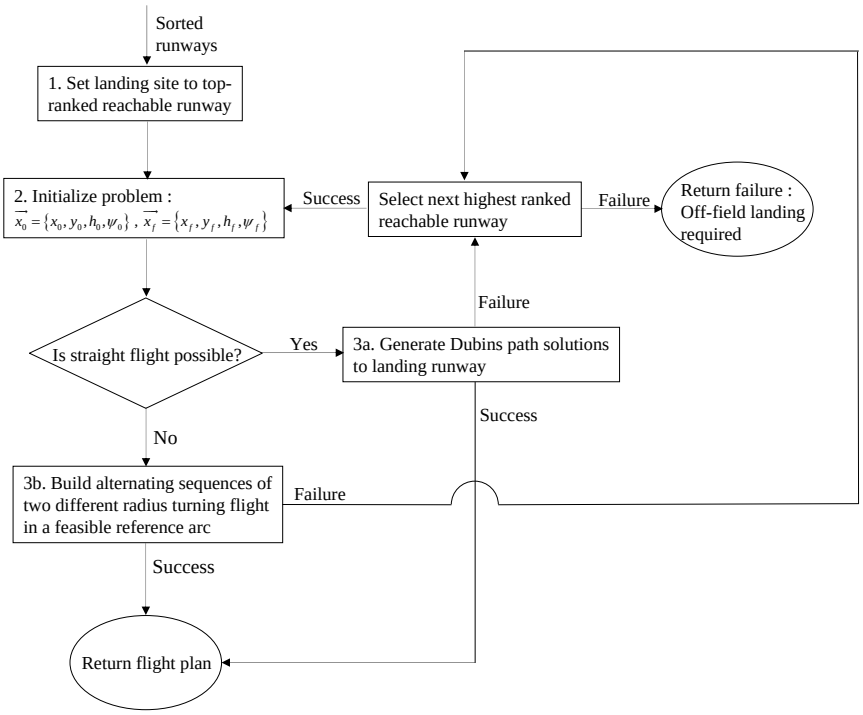

Figure 5. Waypoint Generation Algorithm (WGA)

Since $r_m \leq r \leq r_M$, we can find bounds for $|l_1 - l_2|$. The following lemma bounds this maximum value of J.

Lemma IV.2 *If circular curves of two distinct radii satisfy the condition:*

$$r_1 = r_M \quad and \quad r_2 = r_m \quad if \quad r_1 > r_2 \tag{32}$$

$$r_1 = r_m \quad and \quad r_2 = r_M \quad if \quad r_1 < r_2 \tag{33}$$

then J has the maximum value for all r_r.

Proof Let $r_r \in \mathbb{R}$ and $r_r \geq \frac{\|\vec{r}_{c_f c_i}\|}{2}$. To prove the Lemma, we compute the maximum value of $|2\delta_1 - \delta_2|$ for all r_r, and we maximize the difference between $2\delta_1$ and δ_2. First, consider the case where $r_1 > r_2$. Without loss of generality, let $r_1 = r_M$. As r_2 is varied from r_m to r_M, c_2 converges to c_1 along the line $\overline{p_1 c_1}$ as shown in Figure 2 for $i = 1$. Hence, δ_2 is given by:

$$\delta_2 = \delta_1 - \arctan\left(\frac{\frac{r_M}{2} - r_2}{\sqrt{r_r^2 - \frac{r_M^2}{4}}}\right) \quad \text{if} \quad r_m \leq r_2 \leq \frac{r_M}{2} \tag{34}$$

$$\delta_2 = \delta_1 + \arctan\left(\frac{r_2 - \frac{r_M}{2}}{\sqrt{r_r^2 - \frac{r_M^2}{4}}}\right) \quad \text{if} \quad \frac{r_M}{2} \leq r_2 \leq r_M \tag{35}$$

If $\frac{r_M}{2} \leq r_m$, then we only consider Eq. 35. Since the arc tangent in Eqs. 34 and 35 is nondecreasing for the tangent angle ranging $-\frac{\pi}{2}$ to $\frac{\pi}{2}$, δ_2 has the minimum value if $r_2 = r_m$. Furthermore, since δ_1 is independent of r_2, δ_1 has the maximum value if $r_1 = r_M$. For $r_1 > r_2$, if $r_1 = r_M$ and $r_2 = r_m$, then J has the maximum value for all r_r. Note that since we consider all r_r, r_r depends on the two centers of the initial and final circular curves. Next, we consider the case where $r_1 < r_2$. The second case is the same as the first case setting $r_1 = r_m$ and $r_2 = r_M$. Note that for the second case, δ_2 is given by:

$$\delta_2 = \delta_1 + \arctan\left(\frac{r_2 - \frac{r_m}{2}}{\sqrt{r_r^2 - \frac{r_m^2}{4}}}\right) \tag{36}$$

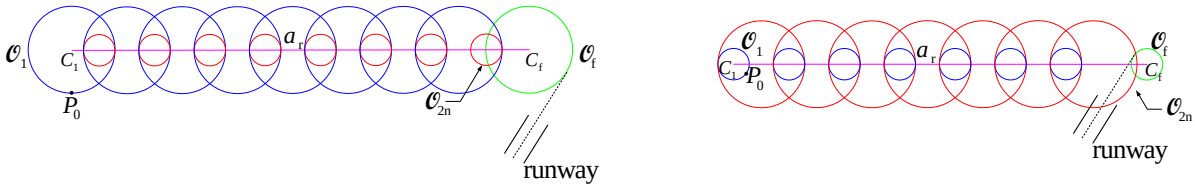

(a) $r_1 > r_2$ (b) $r_1 < r_2$

Figure 6. Determination of n_m

Assume two radii of circular curves satisfy conditions 32 and 33 from Lemma IV.2 for all r_r. Since J is dependent on l_r, $J = |2r_1 - 2r_2|$ for a_r representing straight line. Then the Eq. 31 constraint becomes :

$$\frac{\|\vec{r}_{c_f c_i}\|}{|2r_1 - 2r_2|} \leq n \tag{37}$$

where r_1 and r_2 satisfy conditions 32 and 33 from Lemma IV.2. Since the lower bound in Eq. 37 is in $\mathbb{R}$, but n is in $\mathbb{N}$, $n_m = \lceil \frac{\|\vec{r}_{c_f c_i}\|}{|2r_1 - 2r_2|} \rceil$ where r_1 and r_2 satisfy the conditions 32 and 33 from Lemma IV.2. By Theorem III.1, there exists a_{r_m} such that $\mathcal{O}_{2n}$ and $\mathcal{O}_f$ are tangent at p_{2n}.

The r_r of $a_r \in \mathcal{A}_r$ has range $\frac{\|\vec{r}_{c_f c_i}\|}{2r_r}$ to ∞ according to $\lambda \in [-\infty, \infty]$. However, we have the following constraints on r_r of $a_r \in \mathcal{A}_r$ from Eq. 24 along with $r_r \geq \frac{\|\vec{r}_{c_f c_i}\|}{2}$:

$$r_r \neq 0, \qquad r_r > \frac{r_1}{2}, \qquad r_r \geq \frac{\|\vec{r}_{c_f c_i}\|}{2} \tag{38}$$

Note that r_1 may be greater than $\|\vec{r}_{c_f c_i}\|$ for some cases where $\lambda \in [-\infty, 0)$.

V. Example Landing Trajectories Possible with the TDV Solution

As with our previous work, we adopt a kinematic model to represent flight path displacements of the TDV, i.e. $\mathcal{B}$.[8] In these examples, we ignore the transition between two trim states under the assumption that transient disturbances can be compensated by the guidance and control system in a manner that restores the vehicle to the reference path relatively quickly after the transition is complete. Figure 7 illustrates the families of solutions with lateral plane paths designated by $\mathcal{B} = \{b_i | i \in \{1, 2, \cdots, n_m\}\}$ and a_{r_m} indicated by red dots. Figure 7 satisfies condition 32, and Figure 8 satisfies condition 33. Since the distance between two centers of the initial and final circular curves increases from (a) to (d), as shown in Figures 7 and 8, n_m also increases from (a) to (d). In Figure 7 (a) and (c), λ of the reference arc having n_m is in $[-\infty, 0)$. Note that $r_1 > \|\vec{r}_{c_f c_i}\|$ in Figure 7 (a). Moreover, λ of the reference arc having n_m is in $[0, \infty]$, as shown in Figure 7 (b) and (d). Unlike the case where $r_1 > r_2$, $\lambda \in [0, \infty]$ in Figure 7 (a) to (d). The selected runway can be reached by $\mathcal{B}$ with a_{r_m}, as shown in Figures 7 and 8.

VI. Conclusions and Future Work

This paper has introduced an analytic trajectory planning method in which minimum and maximum-radius turning flight segments are sequenced to safely land a disabled aircraft that can no longer fly along a straight path. The proposed solution covers the comprehensive set of possible initial and final states in the lateral plane. This work complements a traditional Dubins path solver, providing a computationally-efficient (thus real-time) alternative composed only of turning flight segments. Our geometric solution is purposely simple, requiring only two trim states representing maximum and minimum turning radius maneuvers that

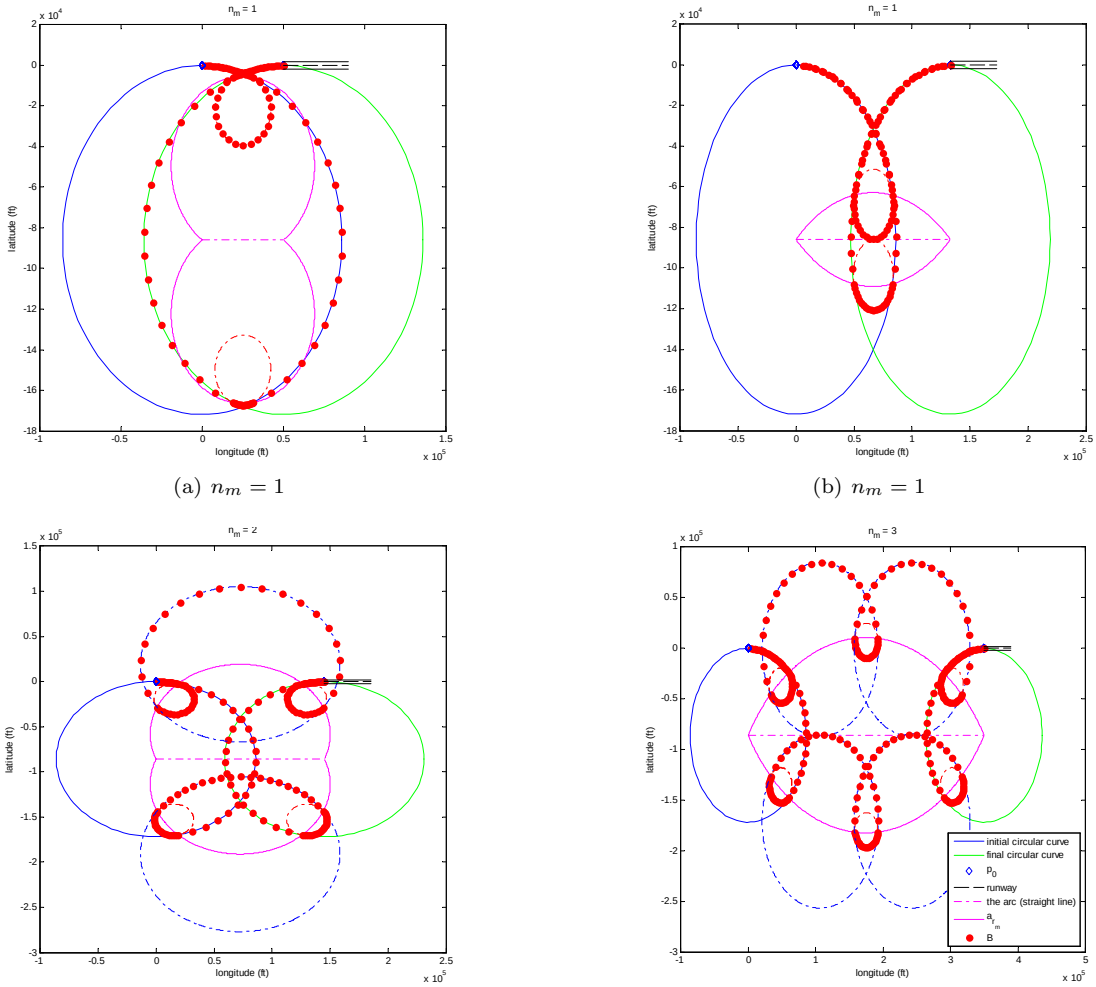

(a) $n_m = 1$ (b) $n_m = 1$

(c) $n_m = 2$ (d) $n_m = 3$

Figure 7. Simulation Results for $\mathcal{B}$ when $r_1 > r_2$

must include a safety factor appropriate for aircraft and environmental conditions. A reference arc a_r defines the path along which a sequence of alternating minimum/maximum radius trimmed (steady) turns are followed.

The proposed analytic trajectory planner is highly computationally efficient compared with existing search-based methods, including that applied to the left wing damage case studied in our previous work.[3] Without search, this work guarantees the shortest-length path to guide the aircraft to the desired touchdown state given the inability to fly straight. However, we currently make two simplifying assumptions that must be fully addressed in future work. First, we ignore configuration changes accumulated during the transition between trim states, i.e., from a state $i-1$ to i. Such transitions have been shown to be nontrivial but will require substantial effort to accurately represent in the purely geometric model we have developed in this work. Second, we presume the longitudinal and lateral aircraft dynamics are fully-decoupled, and that we can achieve a flight path angle that yields the necessary altitude change from initial to final (landing) state. Although this assumption has allowed analysis of landing trajectories strictly in the lateral plane, in future work constraints on flight path angle as a function of turning radius must be respected, potentially requiring an algorithm to automatically extend the minimum-length landing path generated by the TDV solver.

Ultimately, the task of the feedback control system will be to minimize the error between the planned and actual reference trajectory in inertial coordinates. This will require deviation from the "idealized" trim states used by our flight planner, with alterations particularly in reference bank, pitch, and thrust guiding the aircraft back to its inertial path as needed. With real-world disturbances such as wind or induced disturbances such as the ignored transitions between trim states, the centers of the alternating-radius turning sequences

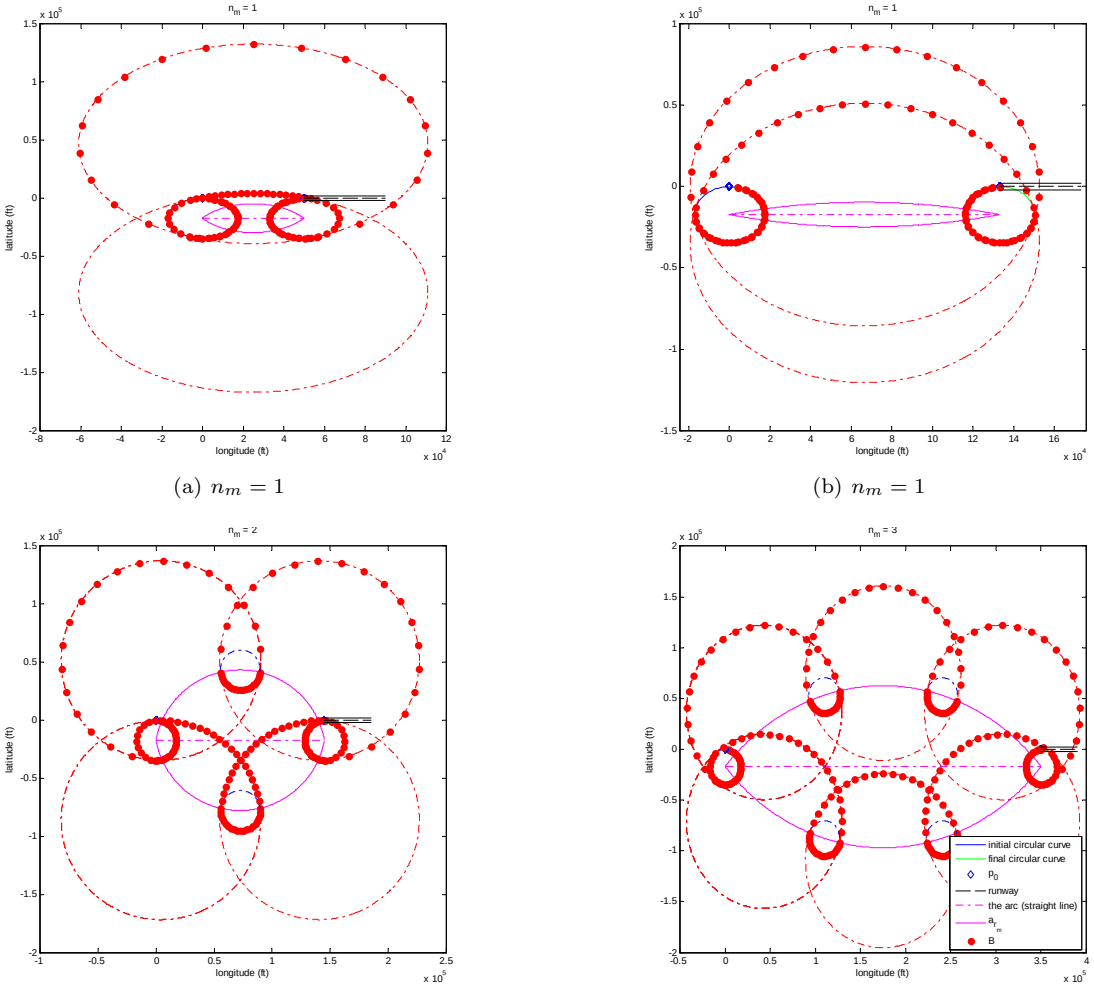

(a) $n_m = 1$ (b) $n_m = 1$

(c) $n_m = 2$ (d) $n_m = 3$

Figure 8. Simulation Results for $\mathcal{B}$ when $r_1 < r_2$

will be shifted in inertial space. Future work is required to anticipate, e.g., through fast-time simulation, situations under which the controller cannot fully-compensate for the suite of disturbances and adjust flight plans accordingly.

References

[1]Atkins, E., Portillo, A., and Strube, M., "Emergency Flight Planning applied to Total Loss of Thrust," *Journal of Aircraft*, Vol. 43, No. 4, Jul-Aug 2006, pp. 1205–1216.

[2]Strube, M., Sanner, R., and Atkins, E., "Dynamic Flight Guidance Recalibration after Actuator Failure," 1st AIAA Intelligent Systems Conference, Sep. 2004.

[3]Tang, Y., Atkins, E., and Sanner, R., "Emergency Flight Planning for a Generalized Transport Aircraft with Left Wing Damage," *Proc. Guidance, Navigation, and Control Conference*, Aug. 2007.

[4]Chen, T. and Pritchett, A., "Development and Evaluation of a Cockpit Decision-Aid for Emergency Trajectory Generation," *Journal of Aircraft*, Vol. 38, No. 5, Sep.-Oct. 2001, pp. 935–943.

[5]Saunders, J., Beard, R., and McLain, T., "Obstacle Avoidance Using Circular paths," AIAA, Guidance, Navigation, and Control Conference, Aug. 2007.

[6]Brinkman, K. and Visser, H., "Optimal Turn-Back Maneuver after Engine Failure in a Single-Engine Aircraft during Climb-Out," *Journal of Aerospace Engineering*, Vol. 221, No. 1, 2007, pp. 17–27.

[7]Boskovic, J., Prasanth, R., and Mehra, R., "A Multi-Layer Autonomous Intelligent Control Architecture for Unmanned Aerial Vehicles," *J. Aerospace Computing, Information, and Communication*, Vol. 1, 2004, pp. 605–628.

[8]Strube, M. J., *Post-failure Trajectory Planning From Feasible Trim State Sequences*, Master's thesis, Aerospace Engineering Dept., University of Maryland, College Park,, 2005.